JOURNAL OF MATERIALS SCIENCE 25 (1990) 4203–4210

Strength–porosity–microstructure relations in porous reaction-sintered SiC with free silicon removed

C.-B. LIM, T. ISEKI
Research Laboratory for Nuclear Reactors, Tokyo Institute of Technology, Ohokayama, Meguro-ku, Tokyo 152, Japan

The effects of controlled porosity on the fracture strength of reaction-sintered SiC (RS-SiC) with free silicon removed and of RS-SiC further heat-treated at 1780° C in a vacuum were investigated. Although further heat-treatment did not cause significant change in porosity of the porous RS-SiC, it was found that the heat-treatment caused strengthening of the porous RS-SiC with below 38% porosity and an intergranular-to-transgranular fracture transition. The strengthening effect may be attributed to increasing bonding area between grains and a relaxation of stress concentration by changing pore shape, resulting from evaporation–condensation and/or surface diffusion by the heat treatment.

1. Introduction

Reaction-sintered silicon carbide (RS-SiC) can be fabricated into fully dense complex shapes without shrinkage during reaction sintering. In this, RS-SiC has an advantage over other structural ceramics and has great potential as a high-performance ceramic.

The major problem impeding the use of RS-SiC as a high-temperature structural material, is its mechanical property, in that the strength decreases because of the loss of strength of silicon as the melting point of 1410° C is approached [1, 2]. On the contrary, the strength of RS-SiC does not decrease further at elevated temperature, because the free silicon has been removed. The strength decrease is obviously caused by pores resulting from the dissipation of free silicon. However, apparently no systematic study exists on this strength–porosity relationship in the porous RS-SiC with silicon removed. In addition, because the RS-SiC is fabricated by a melt-infiltration-type operation into nearly final shape with little, if any, dimensional changes in the presence of a reactive liquid silicon, it is considered that the fracture behaviour of the porous bulk after removal of free silicon is different from that of other porous sintered bodies (e.g. pressureless sintered ceramics), i.e. because of an equilibrium grain-boundary or interfacial configuration between SiC and liquid silicon, determined by their surface energies, the bonding area between SiC grains after removal of free silicon would be expected to have an effect on the strength variations of the bulk, apart from its porosity. It is therefore considered that the porous RS-SiC with free silicon removed should be evaluated not only by strength–porosity relationships, but also by the strength–porosity–microstructure relationships.

The objectives of this work were to systematically and quantitatively investigate the coincident effects of controlled porosity and microstructure on the fracture strength of the porous RS-SiC with free silicon removed, and to describe its microstructural evolution and fracture mode when the porous RS-SiC is further heat treated at 1780° C in a vacuum.

2. Experimental procedure

2.1. Preparation of specimens containing various weight fractions of free silicon

The specimens used in this study were prepared by the method described previously [2–7]. Details of the experiment are given in Table I. The powder mixture of SiC and carbon was pressed into plates of about 30 mm × 30 mm × 6 mm. Table I shows the different SiC : C : phenol resin ratios and compacting pressures applied in order to obtain bulk specimens containing different weight fractions of free silicon. After hardening at 110° C, debonding and carbonization at 1050° C, the compacts were fired in contact with liquid silicon in a graphite crucible with a graphite resistance furnace at 1600° C in a vacuum of 0.65 Pa (4.8×10^{-3} torr) for 30 min. However, only the "IFG 10" specimen was fired at 1450° C for 30 min. The resulting specimens were ground to 4 mm thickness because there was a possibility of structure (e.g. such as shown in Fig. 2d) heterogeneously existing in their surface layer [5–7]. For the "IFG 10" specimen, only one side was ground to 2 mm thick.

These specimens were sectioned parallel to the grinding direction into slices 18 mm long × 4 mm wide × 2 mm thick for preparation of the specimen with free silicon removed, and 1.75 mm thick for the strength measurements of the as-reaction-sintered specimen. The major faces were polished with 1 μm diamond paste in the longitudinal direction with the section planes parallel or with the grinding planes perpendicular (for only the "IFG 10" specimen) to the first uniaxial pressing direction. The density was

0022–2461/90 $03.00 + .12

TABLE I Description of processing conditions and resultant properties of specimens

Specimen number	Processing conditions				Resultant properties	
	Grain size of starting α-SiC filler* (μm)	α-SiC : C† : phenol resin ratio in green compact (by weight)	1st pressing with uniaxial pressure (MPa)	2nd pressing with isostatic pressure (MPa)	Bulk density ($g\,cm^{-3}$)	Free silicon§ (wt %)
A1	1	1:0:0.1	1.5	–	2.63	58
A2			5	–	2.68	52
A3			1.5	150	2.78	41
B4	1	1:0.5:0.15	1.5	–	2.81	38
B5			10	–	2.87	31
B6			10	50	2.98	20
B7			15	260	3.07	13
B8			20	260	3.12	8
C9	7.9	1:0.5:0.15	10	150	3.07	13
IFG 10	7.9	1:0.5:0.15	25	150	3.07	13
SE-10‡	< 5	–	–	–	3.07	13

*GC no. 8000 (1 μm) and GC no. 2000 (7.9 μm) obtained from Fujimi Kenmazai Kogyo Co. Ltd, Nagoya.
†Carbon black (Type Diablack I, 0.02 μm) obtained from Mitsubishi Chemical Industries, Ltd, Tokyo.
‡RS-SiC manufactured by Shinetsu Chemical Co. Ltd, Tokyo.
§Calculated from the bulk density.

determined by Archimedes immersion technique using water. In all cases, from X-ray diffraction (XRD) results, no unreacted carbon was found in the RS-SiC bulk.

2.2. Further heat-treatment after removal of free silicon

Selected samples, given in Table I, were heat treated at 1600° C in a vacuum of 0.65 Pa for 90 min to achieve removal of free silicon. As seen, the final structure of the RS-SiC consists of connected SiC grains, with free silicon occupying the residual pore space necessary for full penetration of liquid silicon into the pressed compact. Nearly complete removal of free silicon is then possible, because the silicons are linked with one another to form a continuous network between the connected SiC grains of the RS-SiC bulk [2, 3]. Evaporated quantities of free silicon were determined from weight changes before and after heat-treatment. In order to determine the amount evaporated, it was assumed that no passive oxidized quantity was included, no decomposited quantity of SiC caused by the heat-treatment, because the presence of free carbon was not detected from XRD results. Furthermore, after free silicon removal, the porous specimens were further heat-treated at 1780° C in a vacuum of 0.65 Pa for 2 h.

The density of the porous specimen was also determined by the same technique mentioned above. The volume fraction porosity was calculated from the density with reference to a theoretical density value of SiC. The complete removal of free silicon was confirmed using the SiC : Si ratio from XRD measurement.

Finally, XRD analyses on the surface of specimens were also carried out to characterize the effects of further heat treatment on these porous specimens.

2.3. Fracture-strength measurement and microstructural observations

The porous specimens for fracture-strength measurement were further ground to a constant thickness of 1.75 mm, from an as-heat-treated surface towards the centre, and their two major surfaces were finally polished with 1 μm diamond paste parallel to the longitudinal direction. The two edges of the tensile surface of the specimens were rounded. Fracture-strength measurements were carried out in four-point bending with an inner span of 7 mm, an outer span of 14 mm, and a cross-head speed 0.5 mm min^{-1}.

The fractured surface was observed with a scanning electron microscope (SEM).

3. Results and discussion

3.1. Microstructural observation before heat-treatment

Typical microstructures containing free silicon from the lowest to the highest weight per cent are shown in Figs 1 and 2. In Fig. 1a, from the SiC : phenol resin (carbonized ratio: 47 wt %) ratio, the theoretical weight per cent of newly formed SiC in the total SiC is 13.6, assuming complete conversion all the carbon to SiC; it was found possible to disperse the primary SiC filler in the compacting and firing. On the other hand, Fig. 1b reveals a fairly uniform dispersion of free silicon. These specimens would thus be expected to behave in an isotropic manner, because the SiC and free silicon distribution were not clustered.

As shown in Fig. 2, the size of free silicon became quite large as the average grain size of the primary SiC filler became large, although the specimens had contained the same weight fraction of free silicon. The morphologies or shapes of free silicon grains, however, remained the same.

The particular microstructure shown in Fig. 2d was initially described by both Sawyer and Page [8] and Ness and Page [9] as consisting of large grains of the primary α-SiC (10 to 20 μm) bonded together by fine β-SiC ($\geqslant 0.5$ μm), which was produced from the reaction of carbon with liquid silicon. They called the fine β-SiC, "intergranular fine-grained β-SiC" (IFG β-SiC). Later, the distribution, behaviour and strength

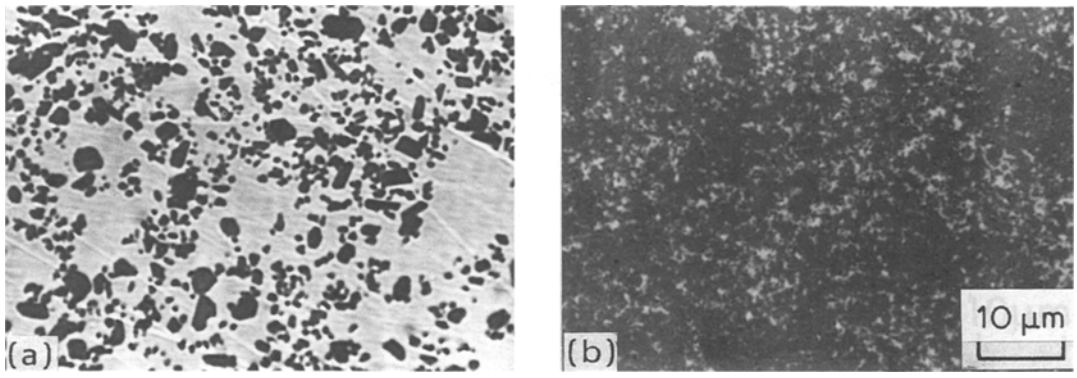

Figure 1 Optical micrographs of as-polished surfaces of (a) specimen A1 containing 58 wt % free silicon, and (b) specimen B8 containing 8 wt % free silicon, showing both SiC (dark) and free silicon (white).

of IFG β-SiC were experimentally and qualitatively investigated by Lim and Iseki [4–7]. As will be discussed later, the fracture strength of the structure containing the IFG β-SiC decrease because of its small bonding area at the grain boundary and an imperfect bonding condition [6, 7].

3.2. Changes in porosity

The porosity data with standard deviation obtained on the heat-treated specimens of the RS-SiC described in Section 3.1 are shown in Table II. The evaporated quantities of free silicon are in agreement with the calculated values shown in Table I. Consequently, it can be regarded that the free silicon in the as-reaction-sintered specimens was nearly all removed by heat treatment at 1600° C. This was confirmed by the XRD results: no silicon peak was detected after heat treatment.

The data show that from the estimated porosity, significant changes in porosity did not occur in most specimens, except for A1 and A2 with some dimensional change, during the removal of free silicon by heat treatment at 1600° C. The decrease in porosity of specimens A1 and A2 corresponded well to the dimensional change (shrinkage) in length (for details, see Section 3.4.2.). In other specimens, however, little or no shrinkage occurred even when the porous specimens with free silicon removed were further heat treated at 1780° C for 2 h. The slight difference in porosity between specimens heated at 1600 and 1780° C may represent either experimental error in density measurements or the presence of a small amount of free carbon which was formed by interfacial reaction and sublimation or decomposition of SiC [10, 11]. The XRD results revealed the absence of free carbon in the 1600° C heated specimens, but the presence of a small amount of free carbon in the 1780° C heated specimens was seen. In particular,

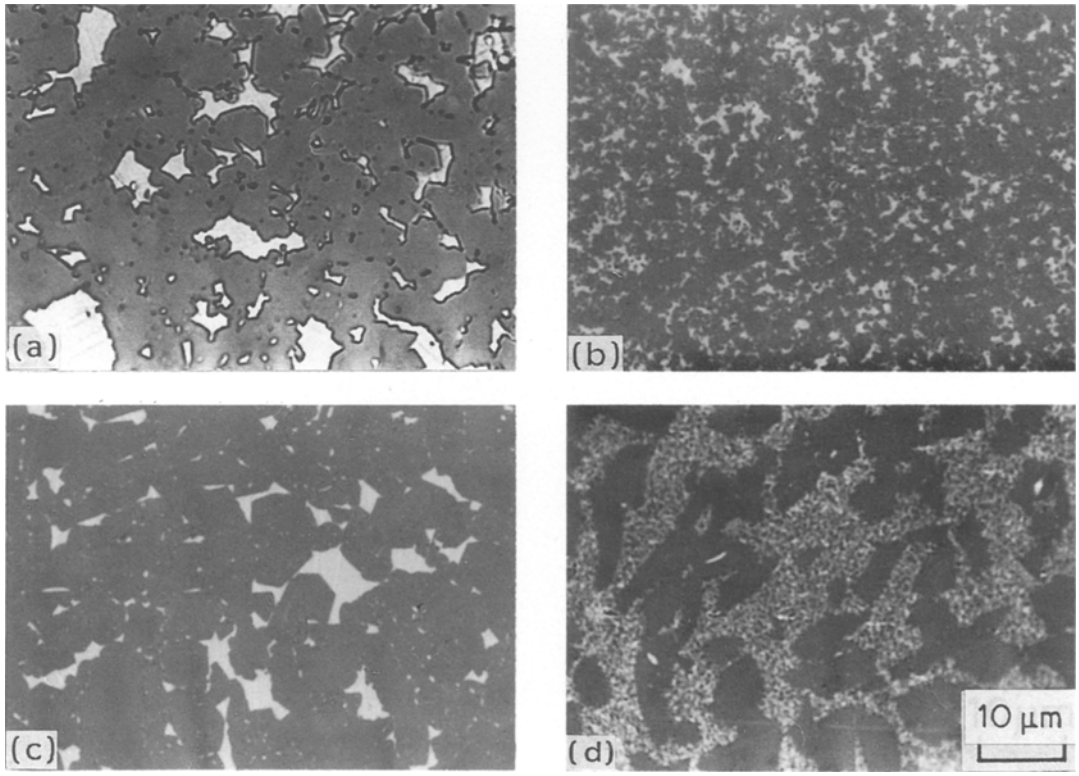

Figure 2 Optical micrographs of as-polished surfaces of various specimens with nearly the same density (about 3.07 g cm^{-3}), containing 13 wt % free silicon: (a) SE-10, B7, (c) C9 and (d) IFG 10. Dark regions are SiC and white regions are free silicon. (d) Typically called the intergranular fine-grained SiC structure in which newly formed fine β-SiC grains with uniform grain size ($\leqslant 0.4\,\mu$m) and equiaxed shape are homogeneously embedded in free silicon between primary α-SiC fillers (7.9 μm).

TABLE II Summary of porosity and dimensional change of specimens after heat treatment in a vacuum

Specimen number	At 1600° C				At 1780° C	
	Evaporated quantity of free silicon (wt %)	Estimated porosity* (vol %)	Observed porosity (vol %)	Linear dimensional change in length (%)	Observed porosity (vol %)	Linear dimensional change in length (%)
A1	60 ± 1	67	58 ± 2	8.1	60 ± 2	8.7
A2	53 ± 2	61	54 ± 1	5.2	54 ± 2	5.5
A3	40 ± 2	48	44 ± 1	0.4	46 ± 2	0.4
B4	38 ± 1	46	44 ± 1	0.1	46 ± 1	0.4
B5	29 ± 1	36	36 ± 1	0.2	38 ± 1	0.4
B6	21 ± 1	27	27 ± 1	0.1	27 ± 1	0.4
B7	12 ± 0	16	17 ± 1	0.1	16 ± 1	0.2
B8	7 ± 0	10	9 ± 0	0.0	9 ± 0	0.0
C9	13 ± 0	17	18 ± 0	0.1	17 ± 0	0.1
IFG 10	13 ± 1	18	18 ± 0	0.2	17 ± 1	0.4
SE-10	13 ± 0	17	19 ± 0	0.1	18 ± 1	0.2

*Calculated from the evaporated quantity of free silicon.

strong graphite peaks appeared for specimens having > 45% porosity (e.g. A1, 2, 3 and B4).

3.3. Effect of porosity on fracture strength

The four-point bending strength as a function of free silicon or pores is shown in Fig. 3 and the strength measurements are summarized in Table III.

The experimental data obtained for the porous specimens by both heat treatments can be represented by an expression of the form [12]

$$\sigma_p = \sigma_{SiC} e^{-nP} \quad (1)$$

where σ_p is the porous SiC body strength, σ_{SiC} the nonporous SiC body strength, P the volume fraction porosity, and n the slope of the ln σ–P curve.

A significant difference in n appeared between the 1600 and 1780° C heated specimens, i.e. n changed from 5 to 4 on further heat treatment after removal of free silicon. Incidentally, when the zero porosity strength values, σ_{SiC}, shown in Fig. 3 are calculated from the conventional composite strength formula

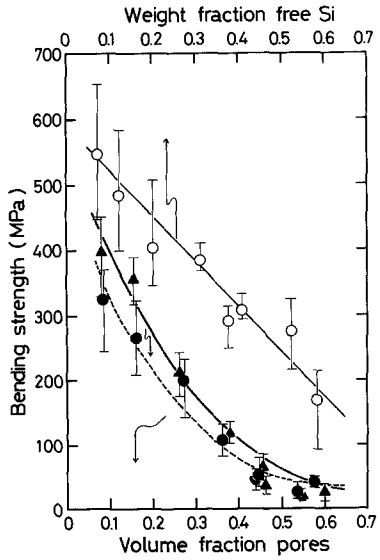

Figure 3 Strength variation as a function of the fraction of free silicon or pores in bulk RS-SiC. The bar indicates the data range. Each point represents at least three individual tests. (—○—) As-prepared, containing free silicon, (- -●- -) heat treated at 1600° C, (—▲—) heat treated at 1780° C.

calculated using a straight line joining the strength of pure silicon (82 MPa in the present experiment) and 89 vol % (92 wt %) SiC (544 MPa) and Equation 1, it has an average strength of 599 and 605 MPa, respectively.

In Table III, the strength of the specimen B7 with the smallest starting grain size tended to be somewhat higher than others after 1600° C heat treatment. This may be closely related to the fracture mode described in the following section. Knudsen [13] indicated that the strength of a porous body decreases with increasing grain size, dealing with simultaneous changes in porosity and grain size. However, Passmore *et al.* [14] reported that it was responsible for the decreasing porosity dependence of strength with increasing grain size and the decreasing grain size dependence with increasing porosity; the strengthening effect would also be expected to increase with increasing pore size and decreasing interpore spacing.

3.4. Examination of fractured surfaces

3.4.1. Grain growth

At 1780° C, grain growth of SiC does not basically occur [2, 15]; this agrees with the results shown in Figs 4a and b. However, slight grain growth occasionally occurred during 1780° C heating, as shown in Figs 4c to h. This could be due to the fact that in the case of a specimen containing grains of a far smaller size than their average size, the smaller grains grow to some limiting grain size close to the uniform grain size, as shown in Figs 4a, b and d, and appear to stop. In fact, in the case of specimens with uniform grain size, as shown in Figs 5a, b, e and f, the grain growth does not occur at least at 1780° C [7, 10, 11].

For IFG SiC shown in Fig. 5g, Lim and Iseki [4–7] reported that the fine SiC grains bonded and coalesced

TABLE III Room-temperature fracture strength of specimens with nearly the same porosity after heat treatment in a vacuum

Specimen number	At 1600° C (MPa)	At 1780° C (MPa)	Percentage increase (%)
B7	265 ± 69	356 ± 37	34
C9	247 ± 38	338 ± 23	37
IFG 10	211 ± 19	327 ± 34	55
SE-10	205 ± 27	322 ± 30	57

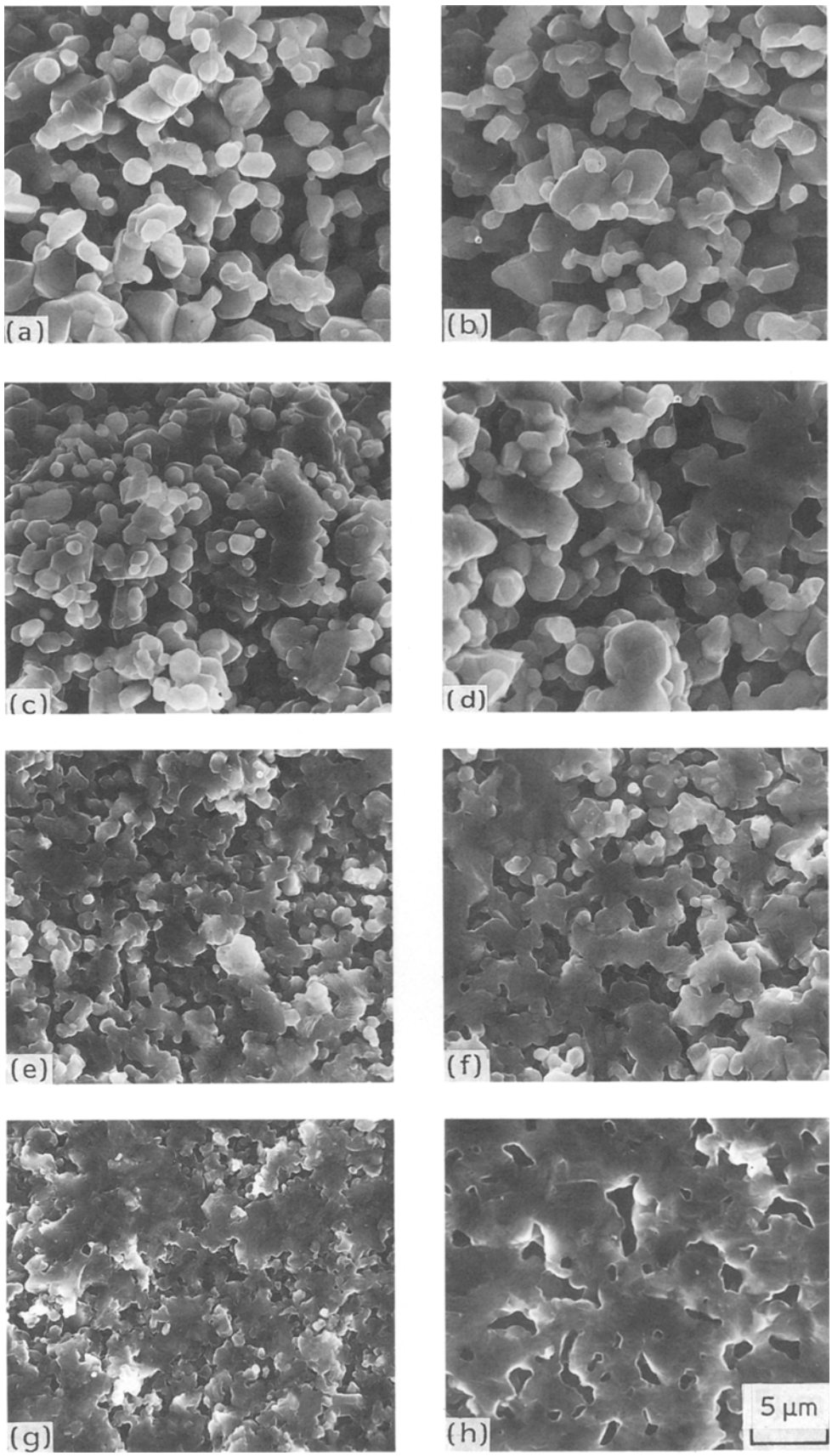

Figure 4 Scanning electron micrographs of fractured surfaces of specimens with various porosities, heat treated at 1600° C (left) and further heat treated at 1780° C (right). (a, b) A1, (c, d) B5, (e, f) B6, and (g, h) B8.

to primary SiC grains by mass transport and migration through liquid silicon, but it was found that the fine SiC grains could substantially coalesce to larger primary SiC grains with grain growth by 1780° C heat-treatment, leaving larger intergranular pores which acted as a sink for smaller pores between the IFG SiC, even though free silicon was absent.

3.4.2. Changes in pore shape and size

The shape of pores in the 1600° C heated specimens

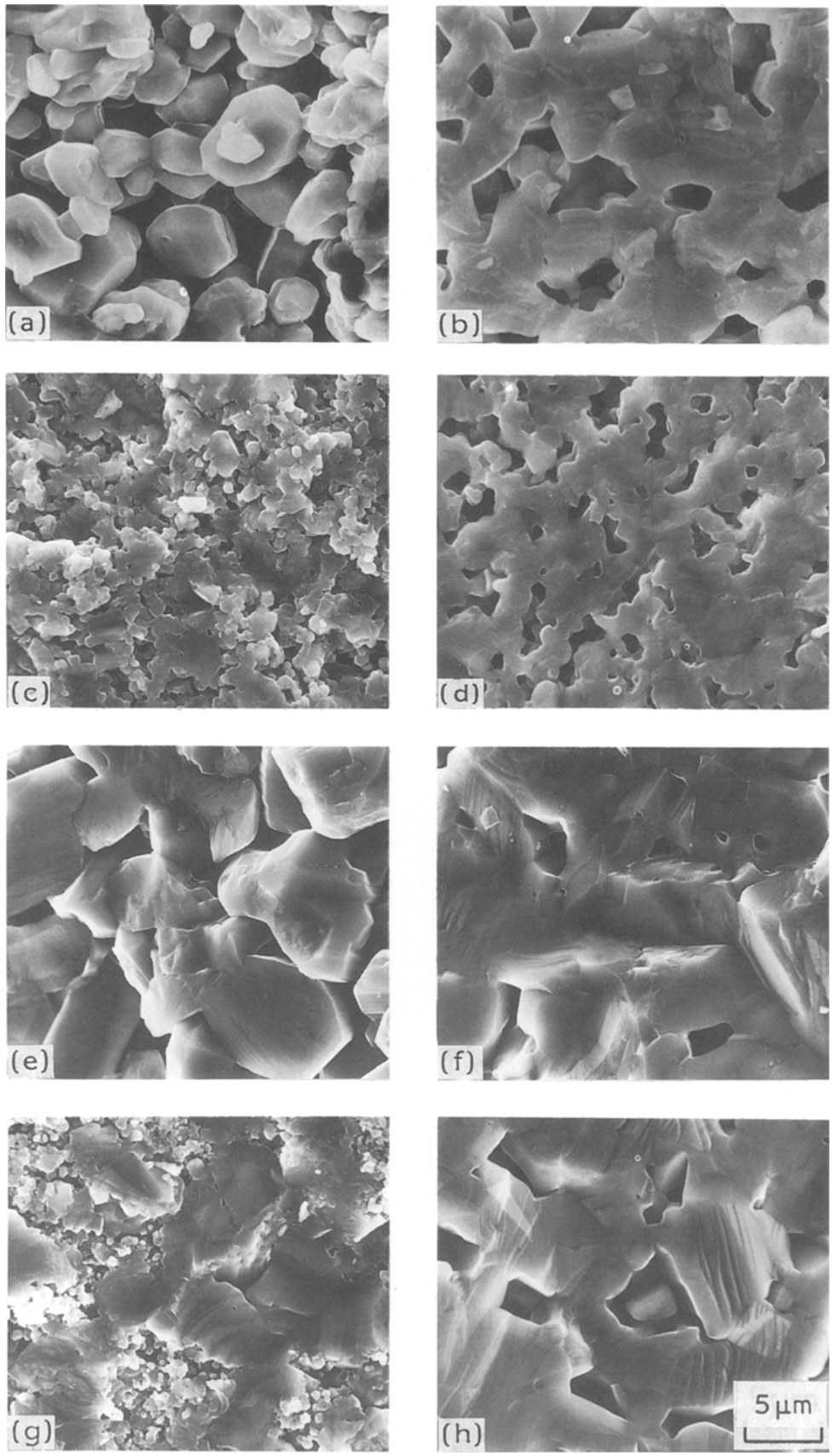

Figure 5 Scanning electron micrographs of fractured surfaces of specimens with nearly the same porosity (17%), heat treated at 1600° C (left) and further heat treated at 1780° C (right). (a, b) SE-10, (c, d) B7, (e, f) C9, and (g, h) IFG 10.

changes to remain smoother and rounder with neck growth or increasing bonding area between the grains on heat-treatment at 1780° C (Figs 4 and 5). Further, the pores in the porous RS-SiC with a uniform grain size do not agglomerate into large pores on heat treatment of 1780° C because no grain growth occurs, as shown in Figs 5a and e. However, the large intergranular pores in the specimen shown in Fig. 5h resulted from the coalescence of IFG SiC which bonded with the primary SiC grains. The pores in the specimens shown in Figs 4 and 5d also tended to agglomerate slightly because the porous specimens

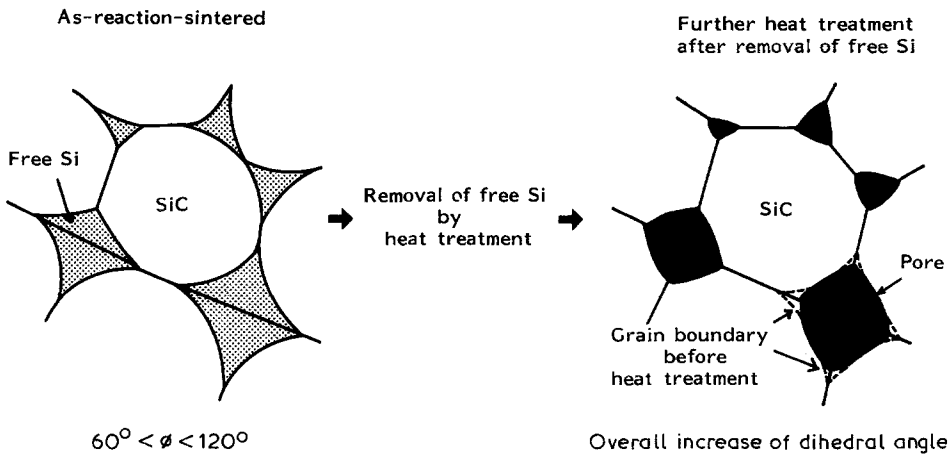

Figure 6 Schematic representation of free silicon distribution and a value of dihedral angle, ϕ, between SiC and silicon in as-reaction-sintered specimen, and changes in pore shape resulting from evaporation–condensation and/or surface diffusion by heat-treatment in a porous specimen.

partly contained grains of a far smaller size than their average grain size.

For the SiC–Si system the dihedral angle, ϕ, depends on the relationship between the interfacial (γ_{SL}) and grain-boundary energies (γ_{SS}) according to the relation

$$\cos \phi/2 = \gamma_{SS}/2\gamma_{SL} = \gamma_{SS}/2(\gamma_{SV} - \gamma_{LV} \cos \theta) \quad (2)$$

where γ_{SV} and γ_{LV} are surface energy of SiC and liquid silicon, respectively. The values of γ_{SS} ($= 1.29\gamma_{SV}$), γ_{SV} ($= 3500\,\text{erg cm}^{-2}$), γ_{LV} ($= 730\,\text{erg cm}^{-2}$), and wetting angle θ ($= 35°$) were taken from data of Grescovich and Rosolowski [16], Inomata and Matsumoto [17], Kingery [18], and Whalen and Anderson [19], respectively. From Equation 2, the value of ϕ is calculated to be about 78°. Consequently, as shown in Fig. 6, the free silicon partially penetrates along the SiC grain intersections at the corners of three SiC grains; when the free silicon is removed, the small bonding area at the SiC grain boundary remains, just as it was. So the porous RS-SiC is subsequently heated at elevated temperature (e.g. 1780° C), the vapour phase and/or surface mass transport occurs from the grain surface to the intergranular neck [10, 11]; the bonding area at the grain boundary increases, as shown in Figs 4 to 6. From a common approximate relationship between the pore with 14 surrounding grains [20] and a pore diameter to grain diameter ratio (about 1), the dihedral angle for a pore stability in the porous RS-SiC with a uniform grain size [5, 10, 11] is about 120°. Therefore, the shape of the pores in the 1600° C heated specimen changes to remain more stable and round on heat-treatment at 1780° C.

In addition, the total shrinkage of porous RS-SiC is unaffected by the evaporation–condensation and surface diffusion (see Table II). Past investigation has revealed a mass transport by surface diffusion in a hot-pressed and annealed β-SiC sintered body at 1900° C without applied pressure; Grescovich and Rosolowski [16] reported that during subsequent annealing at temperatures which permitted sufficient mass transport, high-energy grain boundaries shrank and ultimately caused the breaking of necks between grains having a certain range of mutual orientations, and this process was accompanied by high surface diffusion but no change in bulk density. It seems likely that the shrinkage of specimens A1 and A2 described in Table II is caused by a process similar to that in the initial stage of solid-state sintering, in which the discrete grains link up with one another to form a continuous network by surface diffusion. Hase and Suzuki [21] reported that in pressureless sintering of an SiC compact with about 50% porosity, shrinkage by surface diffusion occurred somewhat at 1400 to 1600° C and appeared to stop.

3.4.3. Intergranular-to-transgranular fracture transition

A microstructural examination by SEM of the fractured surfaces shown in Figs 4 and 5 further elucidated the effects of the heat treatment after removal of free silicon, and offered some indications of what may tend to strengthen the porous RS-SiC.

The fracture mode in most of the 1600° C heated specimens was primarily intergranular, but that in specimen C9 was more transgranular than those in others (Fig. 5e). This may be due to the basis that the fracture mode become predominantly transgranular with increasing grain size. Furthermore, in the 1600° C heated specimens, it may be pointed out that an intergranular-to-transgranular fracture transition occurred slightly with decreasing porosity, showing an increase in bonding area between the grains; the effect was promoted by further heat treatment at 1780° C. The transition resulting from the 1780° C heat treatment began to occur in specimen B5 with 38% porosity; the fracture mode in specimen B8 with 9% porosity became completely transgranular. The transition was not affected by the grain size and pore size, as shown in Fig. 5.

The fracture mode in RS-SiC is primarily transgranular [2, 5, 6, 10, 11], but where there are some pores, as may be seen from the 1600° C heated specimens shown in Figs 4 and 5, the fracture becomes predominantly intergranular. The grain-boundary fracture energy should be less at larger grain sizes than at smaller grains sizes, and than the transgranular fracture energy or cleavage energy [22]. This should be

especially marked in materials with imperfect grain bonding and a small bonding area at grain boundaries. Consequently, the transgranular fracture mode resulting from the 1780° C heat-treatment suggests that the bonding area was significantly increased by the heat treatment and the stress concentration relaxed due to the smooth pore shapes; this contributes to the increase in strength.

Furthermore, most of the interfaces between the newly formed SiC also have pores or inclusions lying along them [5], but these defects are eliminated somewhat by heat treatment; this may also contribute to the increase in strength [10, 11].

This knowledge may have a beneficial effect on the use of SiC bodies as high-temperature components without degradation of strength and the application of an SiC skeleton with free silicon removed to composite materials [2] and organic material filters.

4. Conclusions

When porous RS–SiC with free silicon removed by 1600° C heat treatment was further heat treated at 1780° C in a vacuum, for the specimens with below 38% porosity,

1. the fracture strength increased, showing a change in the slope of the strength—porosity curve and little grain size-dependence of strength; appreciable shrinkage and grain growth did not occur;

2. in most cases, the pores primarily changed in shape rather than size due to evaporation–condensation and/or surface diffusion, showing an increase in bonding area and the dihedral angle between grains, but an obvious agglomeration of smaller pores into larger ones occurred in the specimen with bimodal grain structure (e.g. IFG SiC) as growth of smaller grains proceeded;

3. an intergranular-to-transgranular fracture transition occurred, regardless of grain size and pore size; this is attributed to an increased bonding area between grains. The increase of bonding area and the relaxation of stress concentration by changing pore shapes may contribute to the increase in strength.

References

1. C. W. FORREST, P. KENNEDY and J. V. SHENNAN, "Special Ceramics 5", edited by P. Popper (British Ceramic Research Association, Stoke-on-Trent, 1972) p. 99.
2. C. B. LIM, T. YANO and T. ISEKI, *J. Mater. Sci.* **24** (1989) 4144.
3. T. ISEKI, M. IMAI and H. SUZUKI, *Yogyo-Kyokai-shi* **91** (1983) 259.
4. C. B. LIM and T. ISEKI, *Adv. Ceram. Mater.* **3**(3) (1988) 291.
5. *Idem, ibid.* **3**(6) (1988) 590.
6. *Idem, J. Mater. Sci.* **23** (1988) 3248.
7. T. ISEKI and C. B. LIM, in "Sintering 87", edited by S. Somiya, M. Shimada, M. Yoshimura and R. Watanabe (Elsevier, Tokyo, 1988) p. 1046.
8. G. R. SAWYER and T. F. PAGE, *J. Mater. Sci.* **13** (1978) 885.
9. J. N. NESS and T. F. PAGE, *ibid.* **21** (1986) 1377.
10. C. B. LIM and T. ISEKI, *Seramikkusu Ronbunshi.*, **97** (1989) 1498; *J. Ceram. Soc.*, **98** (1990) 56; *J. Ceram. Soc. Japan*, Int. Ed. **97** 1508.
11. *Idem, ibid. Japan,* Int. Ed. **98** (1990) 58.
12. E. RYSHKEWITCH, *J. Amer. Ceram. Soc.* **36** (1953) 65.
13. F. P. KNUDSEN, *ibid.* **42** (1959) 376.
14. E. M. PASSMORE, R. M. SPRIGGS and T. VASILOS, *ibid.* **48** (1965) 1.
15. S. PROCHAZKA, in "Silicon Carbide 1973", edited by R. C. Marshall, J. W. Faust Jr and C. E. Ryan (University of South Carolina Press, Columbia, 1974) p. 394.
16. C. GRESKOVICH and J. H. ROSOLOWSKI, *J. Amer. Ceram. Soc.* **59** (1976) 336.
17. Y. INOMATA and S. MATSUMOTO, *Yogyo-Kyokai-shi* **79** (1971) 40.
18. W. D. KINGERY, *J. Phys. Chem.* **57** (1953) 359.
19. T. J. WHALEN and A. T. ANDERSON, *J. Amer. Ceram. Soc.* **58** (1975) 396.
20. W. D. KINGERY, H. K. BOWEN and D. R. UHLMANN, "Introduction to Ceramics", 2nd Edn (Wiley, New York, 1975) p. 488.
21. T. HASE and H. SUZUKI, *Yogyo-Kyokai-shi* **88** (1980) 258.
22. R. W. DAVIDGE, "Mechanical Behaviour of Ceramics" (Cambridge University Press, London, 1979) p. 80.

Received 31 May
and accepted 23 October 1989